Meteor Studies in the Framework of the JEM-EUSO Program

G. Abdellaoui[ah], S. Abe[fu], A. Acheli[aa], J.H. Adams Jr.[pd], S. Ahmad[cb], A. Ahriche[ae], J.-N. Albert[ca], D. Allard[cc], G. Alonso[md], L. Anchordoqui[pf], V. Andreev[pe], A. Anzalone[eh,en], W. Aouimeur[aa], Y. Arai[fw], N. Arsene[ja], K. Asano[fg], R. Attallah[ac], H. Attoui[aa], M. Ave Pernas[mc], S. Bacholle[cc], M. Bakiri[aa], P. Baragatti[eo], P. Barrillon[ca], S. Bartocci[eo], T. Batsch[ic], J. Bayer[dd], R. Bechini[el], T. Belenguer[mb], R. Bellotti[ea,eb], A. Belov[kc], K. Belov[pe], B. Benadda[ah], K. Benmessai[ag], A.A. Berlind[ph], M. Bertaina[ek,el,1], P.L. Biermann[db], S. Biktemerova[ka], F. Bisconti[db], N. Blanc[oa], J. Błęcki[id], S. Blin-Bondil[cb], P. Bobik[la], M. Bogomilov[ba], M. Bonamente[pd], R. Boudaoud[aa], E. Bozzo[ob], M.S. Briggs[pd], A. Bruno[eb], K.S. Caballero[he], F. Cafagna[ea], D. Campana[ef], J-N. Capdevielle[cc], F. Capel[na], A. Caramete[ja], L. Caramete[ja], P. Carlson[na], R. Caruso[ec,en], M. Casolino[fx,ei], C. Cassardo[ek,el], A. Castellina[ek,em], G. Castellini[ed], C. Catalano[cd], O. Catalano[eh,en], A. Cellino[ek,em,1], M. Chikawa[fd], G. Chiritoi[ja], M.J. Christl[pg], V. Connaughton[pd], L. Conti[eo,1], G. Cordero[ha], H.J. Crawford[pa], R. Cremonini[el], S. Csorna[ph], S. Dagoret-Campagne[ca], C. De Donato[ei], C. de la Taille[cb], C. De Santis[ei], L. del Peral[mc], M. Di Martino[em], T. Djemil[ac], S.A. Djenas[ah], F. Dulucq[cb], M. Dupieux[cd], I. Dutan[ja], A. Ebersoldt[db], T. Ebisuzaki[fx], R. Engel[db], J. Eser[pc], K. Fang[pb], F. Fenu[ek,el], S. Fernández-González[ma], J. Fernández-Soriano[mc], S. Ferrarese[ek,el], D. Finco[eo], M. Flamini[eo], C. Fornaro[eo], M. Fouka[ab], A. Franceschi[ee], S. Franchini[md], C. Fuglesang[na], J. Fujimoto[fw], M. Fukushima[fg], P. Galeotti[ek,el], E. García-Ortega[ma], G. Garipov[kc], E. Gascón[ma], J. Geary[pd], G. Gelmini[pe], J. Genci[lb], G. Giraudo[ek], M. Gonchar[ka], C. González Alvarado[mb], P. Gorodetzky[cc], F. Guarino[ef,eg], R. Guehaz[aa], A. Guzmán[dd], Y. Hachisu[fx], M. Haiduc[ja], B. Harlov[kb], A. Haungs[db], J. Hernández Carretero[mc], W. Hidber[ha], K. Higashide[fr,fx], D. Ikeda[fg], H. Ikeda[fp], N. Inoue[fr], S. Inoue[fx], F. Isgrò[ef,ep], Y. Itow[fn], T. Jammer[dc], E. Joven[me], E.G. Judd[pa], A. Jung[cc], J. Jochum[dc], F. Kajino[fi], T. Kajino[fl], S. Kalli[af], I. Kaneko[fx], D. Kang[db], F. Kanouni[ag], Y. Karadzhov[ba], J. Karczmarczyk[ic], M. Karus[db], K. Katahira[fx], K. Kawai[fx], Y. Kawasaki[fx], A. Kedadra[aa], H. Khales[aa], B.A. Khrenov[kc], Jeong-Sook Kim[ga], Soon-Wook Kim[ga], Sug-Whan Kim[gd], M. Kleifges[db], P.A. Klimov[kc], D. Kolev[ba], I. Kreykenbohm[da], K. Kudela[la], Y. Kurihara[fw], A. Kusenko[fv,pe], E. Kuznetsov[pd], M. Lacombe[cd], C. Lachaud[cc], H. Lahmar[aa], F. Lakhdari[ag], O. Larsson[fx,na], J. Lee[gc], J. Licandro[me], H. Lim[gc], L. López Campano[ma], M.C. Maccarone[eh,en], S. Mackovjak[ob], M. Mahdi[aa], D. Maravilla[ha], L. Marcelli[ej], J.L. Marcos[ma], A. Marini[ee], K. Martens[fv], Y. Martín[me], O. Martinez[hc], G. Masciantonio[ei], K. Mase[fa], R. Matev[ba], J.N. Matthews[pi], N. Mebarki[ad], G. Medina-Tanco[ha], L. Mehrad[ah], M.A. Mendoza[hd], A. Merino[ma], T. Mernik[dd], J. Meseguer[md], S. Messaoud[aa], O. Micu[ja], J. Mimouni[ad], H. Miyamoto[ek,el], Y. Miyazaki[fc], Y. Mizumoto[fl],

G. Modestino[ee], A. Monaco[ea,eb], D. Monnier-Ragaigne[ca], J.A. Morales de los Ríos[mc], C. Moretto[ca], V.S. Morozenko[kc], B. Mot[cd], T. Murakami[ff], B. Nadji[aa], M. Nagano[fc], M. Nagata[fh], S. Nagataki[fx], T. Nakamura[fj], T. Napolitano[ee], A. Nardelli[eo], D. Naumov[ka], R. Nava[ha], A. Neronov[ob], K. Nomoto[fv], T. Nonaka[fg], T. Ogawa[fx], S. Ogio[fo], H. Ohmori[fx], A.V. Olinto[pb], P. Orleański[id], G. Osteria[ef], W. Painter[db], M.I. Panasyuk[kc], B. Panico[ef], E. Parizot[cc], I.H. Park[gc], H.W. Park[gc], B. Pastircak[la], T. Patzak[cc], T. Paul[pf], C. Pennypacker[pa], M. Perdichizzi[eo], I. Pérez-Grande[md], F. Perfetto[ef,eg], T. Peter[oc], P. Picozza[ei,ej,fx], T. Pierog[db], S. Pindado[md], L.W. Piotrowski[pc], S. Piraino[dd,eh], L. Placidi[eo], Z. Plebaniak[ic], S. Pliego[ha], A. Pollini[oa], E.M. Popescu[ja], P. Prat[cc], G. Prévôt[cc], H. Prieto[mc], M. Putis[la], J. Rabanal[ca], A.A. Radu[ja], M. Rahmani[ag], P. Reardon[pd], M. Reyes[me], M. Rezazadeh[pb], M. Ricci[ee], M.D. Rodríguez Frías[mc], F. Ronga[ee], M. Roth[db], H. Rothkaehl[id], G. Roudil[cd], I. Rusinov[ba], M. Rybczyński[ia], M.D. Sabau[mb], G. Sáez Cano[mc], H. Sagawa[fg], Z. Sahnoune[ab], A. Saito[fj], N. Sakaki[fo], M. Sakata[fi], H. Salazar[hc], J.C. Sanchez[ha], J.L. Sánchez[ma], A. Santangelo[dd], L. Santiago Crúz[ha], A. Sanz-Andrés[md], M. Sanz Palomino[mb], O. Saprykin[kb], F. Sarazin[pc], H. Sato[fi], M. Sato[fs], T. Schanz[dd], H. Schieler[db], V. Scotti[ef,eg], A. Segreto[eh,en], S. Selmane[cc], D. Semikoz[cc], M. Serra[me], S. Sharakin[kc], T. Shibata[fq], H.M. Shimizu[fm], K. Shinozaki[dd], T. Shirahama[fr], G. Siemieniec-Oziębło[ib], J. Sledd[pg], K. Słomińska[id], A. Sobey[pg], I. Stan[ja], T. Sugiyama[fm], D. Supanitsky[ha], M. Suzuki[fp], B. Szabelska[ic], J. Szabelski[ic], H. Tahi[aa], F. Tajima[fe], N. Tajima[fx], T. Tajima[fx], Y. Takahashi[fs], H. Takami[fw], M. Takeda[fg], Y. Takizawa[fx], M.C. Talai[ac], C. Tenzer[dd], O. Tibolla[hf], L. Tkachev[ka], H. Tokuno[ft], T. Tomida[fk], N. Tone[fx], S. Toscano[ob], M. Traïche[aa], R. Tsenov[ba], Y. Tsunesada[fo], K. Tsuno[fx], T. Tymieniecka[ic], Y. Uchihori[fb], M. Unger[db], O. Vaduvescu[me], J.F. Valdés-Galicia[ha], P. Vallania[ek,em], G. Vankova[ba], C. Vigorito[ek,el], L. Villaseñor[hb], B. Vlcek[mc], P. von Ballmoos[cd], M. Vrabel[lb], S. Wada[fx], J. Watanabe[fl], S. Watanabe[fs], J. Watts Jr.[pd], M. Weber[db], R. Weigand Muñoz[ma], A. Weindl[db], T.J. Weiler[ph], T. Wibig[ic], L. Wiencke[pc], M. Wille[da], J. Wilms[da], Z. Włodarczyk[ia], T. Yamamoto[fi], Y. Yamamoto[fi], J. Yang[gb], H. Yano[fp], I.V. Yashin[kc], D. Yonetoku[ff], S. Yoshida[fa], R. Young[pg], I.S Zgura[ja], M.Yu. Zotov[kc], A. Zuccaro Marchi[fx]

[aa] *Centre for Development of Advanced Technologies (CDTA), Algiers, Algeria*
[ab] *Dep. Astronomy, Centre Res. Astronomy, Astrophysics and Geophysics (CRAAG), Algiers, Algeria*
[ac] *LPR at Dept. of Physics, Faculty of Sciences, University Badji Mokhtar, Annaba, Algeria*
[ad] *Lab. of Math. and Sub-Atomic Phys. (LPMPS), Univ. Constantine I, Constantine, Algeria*
[ae] *Laboratory of Theoretical Physics LPT, University of Jijel, Jijel, Algeria*
[af] *Department of Physics, Faculty of Sciences, University of M'sila, M'sila, Algeria*
[ag] *Research Unit on Optics and Photonics, UROP-CDTA, Sétif, Algeria*
[ah] *Telecom Lab., Faculty of Technology, University Abou Bekr Belkaid, Tlemcen, Algeria*
[ba] *St. Kliment Ohridski University of Sofia, Bulgaria*
[ca] *LAL, Univ Paris-Sud, CNRS/IN2P3, Orsay, France*
[cb] *Omega, Ecole Polytechnique, CNRS/IN2P3, Palaiseau, France*

[cc] APC, Univ Paris Diderot, CNRS/IN2P3, CEA/Irfu, Obs de Paris, Sorbonne Paris Cité, France
[cd] IRAP, Université de Toulouse, CNRS, Toulouse, France
[da] ECAP, University of Erlangen-Nuremberg, Germany
[db] Karlsruhe Institute of Technology (KIT), Germany
[dc] Experimental Physics Institute, Kepler Center, University of Tübingen, Germany
[dd] Institute for Astronomy and Astrophysics, Kepler Center, University of Tübingen, Germany
[ea] Istituto Nazionale di Fisica Nucleare - Sezione di Bari, Italy
[eb] Università degli Studi di Bari Aldo Moro and INFN - Sezione di Bari, Italy
[ec] Dipartimento di Fisica e Astronomia - Universit'i Catania, Italy
[ed] Consiglio Nazionale delle Ricerche (CNR) - Istituto di Fisica Applicata Nello Carrara, Firenze, Italy
[ee] Istituto Nazionale di Fisica Nucleare - Laboratori Nazionali di Frascati, Italy
[ef] Istituto Nazionale di Fisica Nucleare - Sezione di Napoli, Italy
[eg] Università di Napoli Federico II - Dipartimento di Scienze Fisiche, Italy
[eh] INAF - Istituto di Astrofisica Spaziale e Fisica Cosmica di Palermo, Italy
[ei] Istituto Nazionale di Fisica Nucleare - Sezione di Roma Tor Vergata, Italy
[ej] Università di Roma Tor Vergata - Dipartimento di Fisica, Roma, Italy
[ek] Istituto Nazionale di Fisica Nucleare - Sezione di Torino, Italy
[el] Dipartimento di Fisica, Università di Torino, Italy
[em] Osservatorio Astrofisico di Torino, Istituto Nazionale di Astrofisica, Italy
[en] Istituto Nazionale di Fisica Nucleare - Sezione di Catania, Italy
[eo] UTIU, Dipartimento di Ingegneria, Rome, Italy
[ep] DIETI, Università degli Studi di Napoli Federico II, Napoli, Italy
[fa] Chiba University, Chiba, Japan
[fb] National Institute of Radiological Sciences, Chiba, Japan
[fc] Fukui University of Technology, Fukui, Japan
[fd] Kinki University, Higashi-Osaka, Japan
[fe] Hiroshima University, Hiroshima, Japan
[ff] Kanazawa University, Kanazawa, Japan
[fg] Institute for Cosmic Ray Research, University of Tokyo, Kashiwa, Japan
[fh] Kobe University, Kobe, Japan
[fi] Konan University, Kobe, Japan
[fj] Kyoto University, Kyoto, Japan
[fk] Shinshu University, Nagano, Japan
[fl] National Astronomical Observatory, Mitaka, Japan
[fm] Nagoya University, Nagoya, Japan
[fn] Institute for Space-Earth Environmental Research, Nagoya University, Nagoya, Japan
[fo] Graduate School of Science, Osaka City University, Japan
[fp] Institute of Space and Astronautical Science/JAXA, Sagamihara, Japan
[fq] Aoyama Gakuin University, Sagamihara, Japan
[fr] Saitama University, Saitama, Japan
[fs] Hokkaido University, Sapporo, Japan
[ft] Interactive Research Center of Science, Tokyo Institute of Technology, Tokyo, Japan
[fu] Nihon University Chiyoda, Tokyo, Japan
[fv] University of Tokyo, Tokyo, Japan
[fw] High Energy Accelerator Research Organization (KEK), Tsukuba, Japan
[fx] RIKEN, Wako, Japan
[ga] Korea Astronomy and Space Science Institute (KASI), Daejeon, Republic of Korea
[gb] Ewha Womans University, Seoul, Republic of Korea
[gc] Sungkyunkwan University, Seoul, Republic of Korea
[gd] Center for Galaxy Evolution Research, Yonsei University, Seoul, Republic of Korea
[ha] Universidad Nacional Autónoma de México (UNAM), Mexico
[hb] Universidad Michoacana de San Nicolas de Hidalgo (UMSNH), Morelia, Mexico
[hc] Benemérita Universidad Autónoma de Puebla (BUAP), Mexico
[hd] Centro de Desarrollo Aeroespacial - Instituto Politécnico National (CDA-IPN), Mexico

[he] Universidad Autónoma de Chiapas (UNACH), Chiapas, Mexico
[hf] Centro Mesoamericano de Física Teórica (MCTP), Mexico
[ia] Jan Kochanowski University, Institute of Physics, Kielce, Poland
[ib] Jagiellonian University, Astronomical Observatory, Krakow, Poland
[ic] National Centre for Nuclear Research, Lodz, Poland
[id] Space Research Centre of the Polish Academy of Sciences (CBK), Warsaw, Poland
[ja] Institute of Space Science ISS, Magurele, Romania
[ka] Joint Institute for Nuclear Research, Dubna, Russia
[kb] Central Research Institute of Machine Building, TsNIIMash, Korolev, Russia
[kc] Skobeltsyn Institute of Nuclear Physics, Lomonosov Moscow State University, Russia
[la] Institute of Experimental Physics, Kosice, Slovakia
[lb] Technical University Kosice (TUKE), Kosice, Slovakia
[ma] Universidad de León (ULE), León, Spain
[mb] Instituto Nacional de Técnica Aeroespacial (INTA), Madrid, Spain
[mc] Universidad de Alcalá (UAH), Madrid, Spain
[md] Universidad Politécnia de madrid (UPM), Madrid, Spain
[me] Instituto de Astrofísica de Canarias (IAC), Tenerife, Spain
[na] KTH Royal Institute of Technology, Stockholm, Sweden
[oa] Swiss Center for Electronics and Microtechnology (CSEM), Neuchâtel, Switzerland
[ob] ISDC Data Centre for Astrophysics, Versoix, Switzerland
[oc] Institute for Atmospheric and Climate Science, ETH Zürich, Switzerland
[pa] Space Science Laboratory, University of California, Berkeley, USA
[pb] University of Chicago, USA
[pc] Colorado School of Mines, Golden, USA
[pd] University of Alabama in Huntsville, Huntsville, USA
[pe] University of California (UCLA), Los Angeles, USA
[pf] Lehman College, City University of New York (CUNY), USA
[pg] NASA - Marshall Space Flight Center, USA
[ph] Vanderbilt University, Nashville, USA
[pi] University of Utah, Salt Lake City, USA
[1] Corresponding authors: Mario Bertaina (E-mail address: bertaina@to.infn.it), Alberto Cellino (E-mail address: cellino@oato.inaf.it), Livio Conti (E-mail address: livio.conti@uninettunouniversity.net)

Abstract

We summarize the state of the art of a program of UV observations from space of meteor phenomena, in the framework of the JEM-EUSO international collaboration. Our preliminary analysis indicates that JEM-EUSO, taking advantage of its large FOV and good sensitivity, should be able to detect meteors down to absolute magnitude close to 7. This means that JEM-EUSO should be able to record a statistically significant flux of meteors, including both sporadic ones, and events produced by different meteor streams. Being unaffected by adverse weather conditions, JEM-EUSO can also be a very important facility for the detection of bright meteors and fireballs, as these events can be detected even

in conditions of very high sky background. In the case of bright events, moreover, exhibiting a much longer signal persistence with respect to faint meteors, preliminary simulations show that it should be possible to exploit the motion of the ISS itself and derive at least a rough 3D reconstruction of the meteor trajectory. Moreover, the observing strategy developed to detect meteors may also be applied to the detection of nuclearites, exotic particles whose existence has been suggested by some theoretical investigations. Nuclearites are expected to move at higher velocities than meteoroids, and to exhibit a wider range of possible trajectories, including particles moving upward after crossing the Earth. Some pilot studies, including the approved Mini-EUSO mission, a precursor of JEM-EUSO, are currently operational or in preparation. We are doing simulations to assess the performances of Mini-EUSO for meteor studies, while a few meteor events have been already detected using the ground-based facility EUSO-TA.
Key words: Meteors, Nuclearites, JEM-EUSO, Mini-EUSO, EUSO-TA

1. Introduction

Since several years an International Collaboration involving several research institutes located in 16 countries of 4 different continents (Europe, Asia, America and Africa) has been working on the development of the JEM-EUSO mission (Adams et al., 2015a), whose main idea is to put a 2-m class telescope aboard the International Space Station (ISS), to carry out nadir-oriented observations of a variety of very rapidly transient physical phenomena.

The project has evolved with time, and it includes now also smaller, pathfinder missions, namely experiments designed to test the observational strategy, and validate the existing technology to be used for the main mission. Among these JEM-EUSO precursors, there are experiments carried out at the EUSO-TA facility (Adams et al., 2015b) and a recently approved ISS-based mission, named Mini-EUSO Ricci et al. (2015).

The main goal of JEM-EUSO is the detection of Extreme Energy Cosmic Rays (EECR, characterized by energy E above 5×10^{19} eV), making use of a

dedicated refractive telescope having 2.5 m diameter lenses, equipped with an UV detector on its focal plane, covering a wavelength interval between 290 and 430 nm. The telescope will be positioned in one of the modules of the ISS, and will carry out nadir observations from a height of about 400 km above sea level on a full Field of View (FOV) of $\sim 60°$. In this configuration, the instrument will detect the secondary light emissions induced by cosmic rays in the atmosphere (fluorescence and Cherenkov light). This mission design also makes it possible the detection of a variety of transient luminous events in the atmosphere (Adams et al., 2015c), including certainly meteor phenomena (Adams et al., 2015d).

The pathfinder mission Mini-EUSO will use the same technologies of JEM-EUSO, but using smaller lenses (25 cm diameter), producing a much coarser spatial resolution and a smaller FOV $\sim 40°$. Mini-EUSO is currently an approved project of ASI and ROSCOSMOS, and will be put aboard in the Russian Service Module of the ISS, looking to the nadir direction through an UV transparent window. The scientific objectives of Mini-EUSO range from cosmic rays to planetary and atmospheric science, including tests of space observation of meteors and fireballs at UV wavelengths.

In parallel to this space program, a ground-based detector, EUSO-TA, has been operating since 2013 at the Telescope Array facility in Utah. Its main purpose is to perform ground-based tests of the planned observational technique and instrumentation of JEM-EUSO. During some preliminary campaigns of cosmic ray observation, a few meteor events have been already detected, confirming the expectations.

The paper is organized as follows. Section 2 and 3 will briefly report on the concept of the JEM-EUSO and Mini-EUSO detectors and their expected performance for meteor and nuclearite detection, the latter being exotic particles which have been suggested by some theoretical investigations to address the dark matter issue De Rujula and Glashow (1984). Section 4 will summarize the ongoing efforts to implement into ESAF Berat et al. (2010), the software package employed by the JEM-EUSO collaboration, the basic properties of meteor phenomena and the necessary procedures for the detection of their signals

using the JEM-EUSO and Mini-EUSO instruments. Section 5 will show the first examples of meteor tracks detected by means of the JEM-EUSO observational approach, using the EUSO-TA experiment in Utah.

2. JEM-EUSO

An extensive review of the JEM-EUSO concept, including detailed descriptions of the whole instrument hardware, has been published in a special issue (Volume 40, November 2015) of the journal Experimental Astronomy. Here, we briefly recall only the most essential elements.

The system consists of four major parts: (1) collecting optics; (2) focal surface detector; (3) on-board electronics; (4) lodgement structure. In practical terms, JEM-EUSO can be conceived as a large aperture and extremely-fast digital camera with a large field of view, specifically designed to detect extremely rapid events of light emission at UV wavelengths. As mentioned above, the optics consists of a telescope having a diameter of about 2.5 m and a field of view of 60°. The detector is a $\sim 3 \times 10^5$ pixels camera which is able to record incoming radiation at a frequency of 2.5 $\sim$ μs. The whole system operates at wavelengths between 290 and 430 nm, in both single-photon-counting and charge integration modes.

Two curved double-sided Fresnel lenses having an external diameter around 2.5 m, a precision middle Fresnel lens and a pupil, constitute the optics of the telescope. The Fresnel lenses provide a large-aperture, wide FOV optics with low mass and high UV light transmittance. The resulting angular resolution is 0.075°. This corresponds to a linear size of about 550 m on the ground (at nadir) We remind that the ISS orbits at a height of about 400 km. The corresponding resolution for observation of sources located at a height of 100 km above the ground, typical of meteor events, is about 400 m.

The incident UV photons are focused by the optics into the focal surface, where the detector converts them into electric pulses. The focal surface has a spherical shape, about 2.3 m in diameter with a curvature radius of about 2.5 m.

On this surface, about $5,000$ multi-anode photomultiplier tubes (MAPMT) Hamamatsu R11265-03-M64 (1 inch in size, with 8×8 pixels) are located. The detector consists of Photo-Detector Modules (PDMs), each one including Elementary Cells (ECs) consisting of 4 units of MAPMT. A total of 137 PDMs are arranged on the focal surface. A Cockcroft-Walton-type high-voltage supply is used to reduce power consumption. It includes a circuit to protect the photomultipliers from sudden light bursts, such as lightning or bright fireball phenomena.

The on-board electronics records the signals generated by UV photons. A front-end ASIC fulfills both functions of single photon counting and charge integration in a 64 channels chip. The electronics is configured in three levels corresponding to the hierarchy of the focal surface detector: front-end electronics at EC level, PDM electronics common to 9 EC units, and focal surface electronics to control 137 units of PDMs. The anode signals from the MAPMT are digitized at time intervals (named Gate Time Units, GTU) of $2.5\,\mu$s and held in ring memory to wait for a trigger assertion. After the trigger, the data are sent to control boards. JEM-EUSO uses a hierarchical trigger method to reduce the data rate of $\sim 10\,$GB/s down to 297 kbps, required for transmission from the ISS to the ground operation center.

In this way, the pulses produced by incident UV photons are read and recorded by the on-board electronics. Whenever a signal pattern is detected, this triggers the start of a sequence of recording operations which involve a selected pixel region on the detector. The recorded signal data are eventually transmitted to the ground operation center.

2.1. Meteors

The main results of a preliminary investigation of the expected performances of JEM-EUSO for what concerns meteor detection, including also a study of the best possible observation strategy to optimize the results, have been published by Adams et al. (2015d). Here, we will briefly summarize the current situation, while interested readers will find more details in the above-mentioned paper.

The analyses have been based on a simulation software developed to mimic the expected signals produced by meteors on the focal plane of JEM-EUSO in a wide range of possible situations. In particular, any given phenomenon is described by a number of free parameters, including the beginning height of the meteor, the module and direction of its velocity vector, the duration of the event, and the morphology of the light-curve produced by the ablation phase experienced by the meteoroid during its fall through the atmosphere. The simulator is very simple, and no deceleration of the meteoroid has been taken into account so far. Since the photometric behaviour of meteors is very variable and essentially unpredictable a priori, the software has been written in such a way as of being able to produce a large variety of possible light-curves, the signal being approximated by a polynomial of 9^{th} degree. Taking into account that real meteors exhibit often the presence of secondary light bursts along the trajectory, but on the other hand it is not possible to include all the huge variety of possible situations, in its current version the meteor simulator allows for the presence of only one possible secondary light burst, and takes as other free parameters the time when this possible secondary burst occurs, its light-curve morphology and the duration of the secondary burst. In practical terms, the simulations performed so far have assumed some simple light-curve morphology for both the main event and the secondary burst, both being approximated by a polynomial characterized by a raise to a maximum, and subsequent decay. The maximum of the light-curve is another free parameter of the numerical simulator. The computation of the signal is performed by considering two possible observers: one, located on the ground in a fixed location, and another aboard the moving ISS. The varying distances between the meteor and each observer are obviously taken into account in computing the number of photons produced on the focal plane at each instant. In particular, the simulator computes the received signal at time steps of 1 ms. The number of UV photons, computed by taking into account a fixed conversion from apparent UV magnitudes to photon flux, as well as the location of the received signal on the focal plane, is also computed at each time step.

The simulator described above is very simple, yet it allows us to make several useful computations. As an example, it makes it possible to simulate the behaviour of light sources on the terrestrial surface (simulated as meteors at an height of zero km and with zero velocity).

In terms of meteor detection procedures, the results of the simulated signals have suggested a general strategy, based on the idea of using different modes of detection, depending on the apparent luminosity of the events, that can vary over a very large interval. Two main techniques for signal measurement are possible, namely photon counting and charge-integration. Photon counting is the standard procedure for the measurement of cosmic ray events, but it is not suitable to record events producing more than a few tens of photo-electrons per pixel per gate time unit (GTU). At higher rates, charge integration becomes the only possible option (Adams et al., 2015d). Simulations performed so far, including also a number of blind tests, in which the reconstruction of the detected signal was performed without any a priori knowledge of the properties of the simulated event, have shown that a satisfactory reconstruction of the true signals, starting from the recorded photo-electron counts obtained in a large variety of situations, can be achieved.

According to the results obtained so far, and summarized in Table 1, (where we also include some results corresponding to the Mini-EUSO case, see Section 3) we can conclude that JEM-EUSO should be able to detect meteors as faint of absolute magnitude around +7, in conditions of dark background. Another very interesting result was obtained concerning very bright meteor events, usually indicated as *fireballs*. In particular, fireballs reach very bright magnitudes that make them observable in conditions of bright background, the brightest events being visible even in full day.These events are particularly interesting because they involve meteoroids having masses larger than tens of grams. They are so bright that for them the light emitted in most points of the trajectory is not practically instantaneous like in the case of fainter meteors, but it exhibits some persistence over time. As a consequence, many points of the trajectory can be observed for consecutive time steps on the focal plane of the ISS, with a

Table 1: For some different values of absolute magnitudes in visible light, the Table lists the corresponding flux in the U-band (according to the Flux Density Converter of the Spitzer Science Center available at web site http://ssc.spitzer.caltech.edu/warmmission/propkit/pet/magtojy/index.html), the corresponding numbers of photons per second (assuming that the meteor is located at a height of 100 km and is observed by the ISS in the nadir direction), and the corresponding number of photo-electrons per GTU, for the cases of JEM-EUSO and Mini-Euso, respectively. The corresponding typical mass of the meteor, and the number of events expected to be observed by JEM-EUSO (by assuming a duty cycle of 0.2) and by Mini-EUSO are also shown. The relationship between mass and magnitude has been obtained following Robertson and Ayers (1968).

Abs. mag	U-band flux (erg/s/cm^2/A)	photons (s^{-1})	photo-e$^-$ GTU^{-1} (JEM)	photo-e$^-$ GTU^{-1} (Mini)	mass (g)	event rate (JEM)	event rate (Mini)
+7	$6.7{\cdot}10^{-12}$	$4.3{\cdot}10^{7}$	4	0.04	$2{\cdot}10^{-3}$	1/s	0.4/s
+5	$4.2{\cdot}10^{-11}$	$2.7{\cdot}10^{8}$	23	0.23	10^{-2}	6/min	2.4/min
0	$4.2{\cdot}10^{-9}$	$2.7{\cdot}10^{10}$	2300	23	1	0.27/orbit	0.11/orbit
-5	$4.2{\cdot}10^{-7}$	$2.7{\cdot}10^{12}$	$2.3{\cdot}10^{5}$	2300	100	6.3/year	2.5/year

progressive drift across the FOV due to the motion of the ISS. This means that for these objects, by means of some simple trigonometric computations, a 3D reconstruction of the trajectory becomes possible. This also means to be able to compute the original heliocentric object of the meteoroid and, in case of objects sufficiently massive to reach the ground, to constrain the region where the freshly fallen meteorite should be searched for. This is an extremely important result for the study of the origin, composition, and evolution of these celestial bodies.

We did some very preliminary computations of the possible reconstruction of the 3D trajectory of a meteor by measuring the recorded drift of the signal corresponding to three points, only, of the luminous track. The results suggest that, in the case of meteors having an absolute magnitude of the order of +3, the module of the velocity vector of the meteor can be computed with an accuracy of the order of 15% or better. The corresponding 3D coordinates of the meteor head can also be derived with a similar accuracy, the best results corresponding to the choice of the brightest points of the meteor track, which produce a longer drift on the focal plane (see also Fig. 1, in which four different damping coefficients of the meteor signal are considered).

2.2. Nuclearites

Another possible application of JEM-EUSO is the detection of completely different, but extremely interesting luminous sources, the so-called nuclearites. As explained in the quoted Adams et al. (2015d) paper, the possible existence of nuclearites, which could be constituents of dark matter, is predicted by some theoretical studies (De Rujula and Glashow , 1984). Nuclearites are thought to be nuggets made of massive nuclear particles including strange quarks among their constituents. This nuclear matter would be expected to have a small positive electric charge, but neutrality should be assured by the presence of a cloud of surrounding, captured electrons (see, again, De Rujula and Glashow , 1984). According to a number of reasons summarized by Adams et al. (2015d), the absolute magnitude M of nuclearites should depend only on their mass and

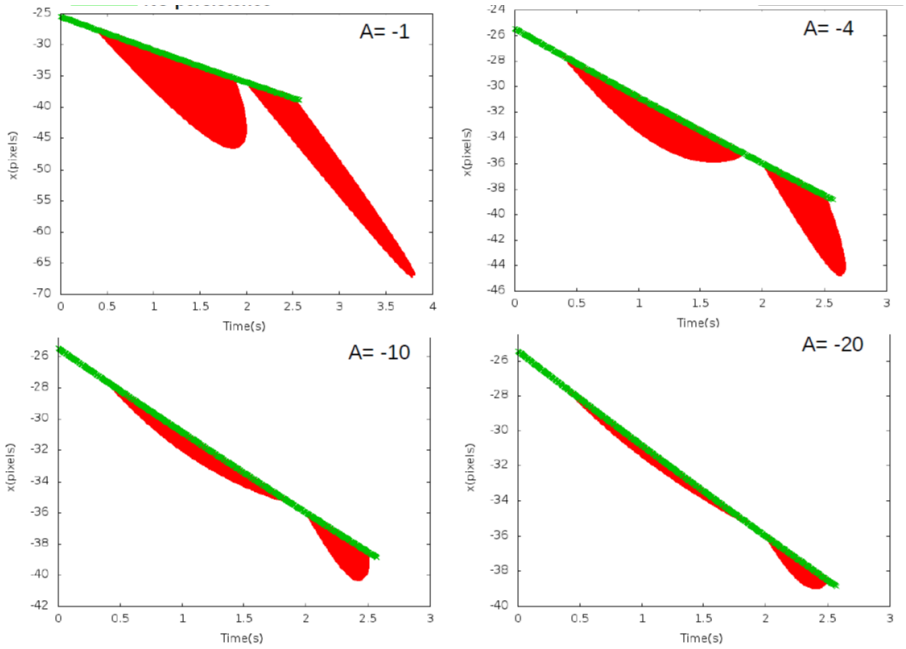

Figure 1: Example of a bright meteor (absolute magnitude $M = 3$ at maximum brightness) producing different signals on the focal plane, depending on the assumed persistence of the signal. Assuming that each point of the meteor light track has an intensity decaying according to the relation $I(t) = I_0 \cdot e^{At}$, with A being a damping coefficient expressed in units of s^{-1}, the Figure shows the expected behaviour for four possible values of A. The light-curve of the meteor, in this particular case, is assumed to exhibit a strong secondary burst. The green line in the four cases shows the x-axis location of the meteor head measured in pixels on the focal plane, as a function of time (the reference frame is centered at the center of the focal plane, the x and y axes being horizontal and mutually perpendicular, while the z axis is oriented toward the nadir direction). The length of the green line is identical in the four cases, but it appears different due to the change of the scale in both axes of the different plots, needed to include the whole region of the position versus time plane occupied in the different cases by the drifting signal (in red) produced by the persistence of the light emitted by each point of the meteor track, depending on the chosen value of the damping coefficient.

should be constant, according to the relation:

$$M = 15.8 - 1.67 \log(m)$$

where m is the mass expressed in μg units. Also interesting is the prediction that the light flux should be emitted only up to a maximum height h_{max}, which is mass-dependent. According to current expectations, most nuclearites should emit only a faint radiation at heights not exceeding a few km, but very massive nuclearites might exist, having masses up to 10^4 g. Such objects could be visible up to about 60 km of height, and have absolute magnitudes $M < 0$.

Nuclearites are expected to move at galactic speeds, up to 570 km/s, significantly higher than meteor velocities, but still in the range of slow events for the JEM-EUSO detector. The big difference with respect to meteors is that nuclearites more massive than 0.1 g are expected to have the possibility to pass freely through the Earth, so some of them, in particular the most massive ones according to previous considerations, could be even observed as very fast meteor-like events moving upward. In spite of the absence in the literature of records of meteor events having such anomalous trajectories, and taking also into account the large nuclear masses required to produce detectable events, the possible observation of nuclearites by JEM-EUSO remains a fairly remote, but extremely exciting possibility. JEM-EUSO is sensitive to strangelet nuclearites with mass $m > 10^{22}$ GeV (see Fig. 2). A null observation of these events will set orders of magnitude more stringent limits than current flux limits Adams et al. (2015d).

3. The Mini-EUSO pilot mission and meteor observation

As mentioned above, Mini-EUSO is an approved pilot mission aboard the ISS, to test the main mission concepts developed for JEM-EUSO. Originally born as a joint project between the national scientific communities of Italy and Russia, Mini-EUSO was selected in Italy by the Italian Space Agency (ASI) and under the name "UV atmosphere", it was approved by the Russian Space Agency (ROSCOSMOS) and included in the long-term program of ISS-based space experiments. Currently, Mini-EUSO is an established project in the framework of the whole JEM-EUSO Collaboration.

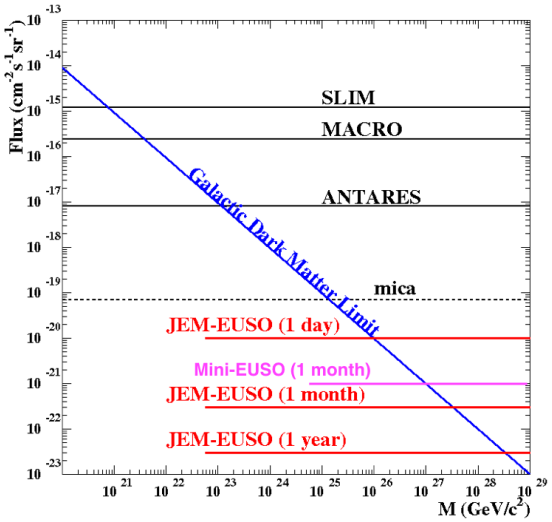

Figure 2: The JEM-EUSO 90% confidence level upper limit on the flux of nuclearites resulting from null detection over 24 hours, 1 month and 1 year of JEM-EUSO operations. The limit for Mini-EUSO is reported only for 1 month operation. For the other durations, they can be rescaled similarly from JEM-EUSO ones. The limits of other experiments Ambrosio et al. (2000), Cecchini et al. (2008), Pavalas et al. (2012), Price (1988) are also shown for a comparison. The old mica limits Price (1988) are dependent on several additional assumptions, with respect to the other experiments.

The Mini-EUSO instrument, whose scheme and conceptual design are shown in Fig. 3, is composed of one single element of the basic detection unit conceived in the JEM-EUSO design, namely the Photo Detector Module (PDM). It consists of 36 Hamamatsu Multi Anode Photo Multiplier Tubes (MAPMT M64), 64 pixels each, for a total of 2304 pixels. The optical system consists of two Fresnel lenses, both having a diameter of 25 cm. The front-end electronics is based, opportunely rescaled, on the same concept of photon-counting technique developed for JEM-EUSO. According to current plans, two visible cameras should also be installed as ancillary instruments to complement the UV detections performed by the Mini-EUSO focal assembly. The Mini-EUSO instrument will be inserted in a specific container, a mechanical box providing

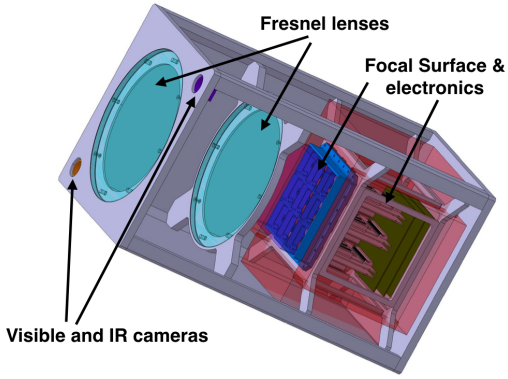

Figure 3: A three dimensional representation of the Mini-EUSO instrument payload.

also all the needed interfaces to the transparent, nadir looking UV window of the Zvezda Russian module aboard the ISS.

The FOV of Mini-EUSO will be about $\pm 20°$, therefore $\sim 0.8°$ per pixel, corresponding to a radius at ground of ~ 150 km. The trigger system and data acquisition is organized in different time scales. For what concerns meteor observation, Mini-EUSO will continuously record data with 40 ms time resolution. Meteor detection and tracking will be performed on ground after data recovery. However, triggers on board with allow to record also portions of the tracks with time resolutions of 2.5 μs and 320 μs, respectively. The same simulator used to evaluate JEM-EUSO performance has been adapted to the Mini-EUSO instrument to get a first estimation of its performance. Thanks to the possibility of performing data reduction on ground, Mini-EUSO sensitivity can reach magnitudes around +4 and +5 in optimal dark-background conditions. In such condition the signal, integrated at steps of 40 ms will exceed by 3-4σ the expected UV-nightglow level. Every year, Mini-EUSO will be able to collect a statistics of meteor signals that should be three times less than that expected for JEM-EUSO. The quality of the recorded meteor tracks will be also worse as the FOV per pixel is 10 times bigger compared to JEM-EUSO. However, in spite of these limitations, it will be still possible to prove the observation principles and strategy conceived for meteor observations by JEM-EUSO.

Regarding the observation of nuclearites, the limits for null observation at a first order of approximation can be rescaled from JEM-EUSO results by simply taking into account both the ratio of the optics, which *per se* shifts the limit on the detectable mass size of the nuclearite by two orders of magnitude, and the ratio of the FOV, which decreases the rate of events by a factor ~ 2.5 (see Fig. 2). Also the quality of track will be worse in Mini-EUSO, but thanks to the higher speed of these objects the total number of pixels crossed by the signal will increase by a factor of a few, so improving considerably the quality of the recorded track compared to the case of a meteor moving along the same direction.

4. Implementation of meteor simulations in ESAF

The performance of JEM-EUSO and Mini-EUSO has been so far evaluated using a simple numerical simulator of meteor phenomena, as described in Section 2. Currently, there is an on-going effort to include this already developed software in the ESAF (EUSO Simulation and Analysis Software) package. The reason is that ESAF is the official software tool to perform simulations of extended air shower (EAS) development of cosmic ray, photon production and transport through the atmosphere, and detector response for optics and electronics. Moreover, ESAF includes also algorithms and tools for the reconstruction of the properties of air showers produced by extremely energetic cosmic rays. Originally developed for the EUSO-ESA mission, all the necessary steps have been taken in recent times to implement in ESAF all the planned JEM-EUSO, Mini-EUSO and EUSO-TA instrumental configurations, in order to assess the full range of expected performances for cosmic ray observation Bertaina et al. (2014). It is therefore important to implement in ESAF also the possibility to carry out detailed simulations of much slower events, taking into account the large variety of possible signals produced by meteors.

In fact, cosmic ray phenomena are much shorter in time, typically a hundred μs, with respect to meteor phenomena that can last up to a few seconds (see

Property	Bright EHECR event	Faint Meteor event
Energy/Magnitude	E = 10^{20} eV	Abs. M = +5
Speed	3×10^5 km/s	20 km/s
Emitted Photons	10^{16}	10^{19}
Photons on pupil	10^4	10^8
Duration	200 μs	2 s

Table 2: Comparison between a typical cosmic ray and a meteor event. The difference in the ratio between the photons at the pupil and those emitted by the two kinds of event takes into account the differences in the distance from the observer and the differences in atmospheric absorption.

Table 2 for a comparison of the main characteristics of the two phenomena). The typical signal expected at the pupil level for a 10^{20} eV extensive air shower is of the order of a few thousands photons in a hundred μs. For each photon it is necessary to track the trajectory through the detector at a ns time resolution. Such brightness on the same time scale corresponds to a meteor of magnitude $M = +5$. However, in case of meteors, the signal duration is expected to be around 4 orders of magnitude longer. This is not a trivial issue from the run-time memory and data output size of the event. Therefore, it is important to adapt ESAF to the simulation of much longer events, lasting up to a few seconds. So far, the way to overcome the problem has been to simulate only a few bunches of light along the meteor track to follow its evolution. A detailed explanation of the method is reported in Nardelli (2014). Moreover, ESAF includes now also an implementation of a formula by Jacchia (Jacchia et al. , 1967) which links the magnitude, mass and the velocity of the meteoroid. Given the meteor's velocity and magnitude, that are free parameters in the simulations, one can therefore derive the corresponding mass of the meteoroid. By assuming a value of density ρ (so far a fixed value $\rho = 3.55$ g/cm^3 has been assumed in preliminary tests) it is possible to compute also the corresponding size of the meteoroid.

Fig. 4 shows an example of a meteor track having absolute magnitude $M = +5$ crossing the FOV of JEM-EUSO with a 60° inclination with respect to the

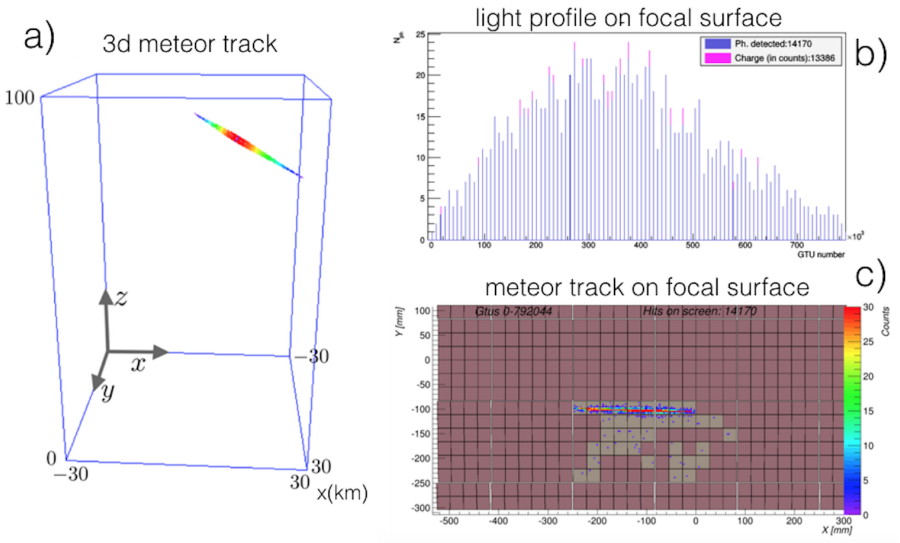

Figure 4: Example of a meteor track of absolute magnitude $M = +5$ simulated with ESAF. a): the 3D trajectory of the meteor in the atmosphere. The zenith angle is 60° from nadir axis. b): the expected light profile on the detector. Only a few GTUs are simulated. c): the resulting meteor track on the focal surface.

nadir axis. Only a few GTUs have been simulated along the track to solve the memory and data size of the output file issues. At the peak of light the expected number of counts is around 20 per GTU. This confirms the results presented in Table 1, where the detector response was parametrized. The UV night-glow is not simulated, however. In case of dark nights without moon the background is estimated to be of the order of 1 count/pixel/GTU.

The possibility of generating secondary light bursts of a meteor as well as simulating the light persistence has been now implemented in ESAF. Fig. 5 shows an example for both cases. The absolute magnitude of the meteor is $M = +5$ with a duration of 2 s. The secondary burst has a magnitude of $M = +3$ with a duration of 0.5 s, starting 1.5 s from the beginning of the event. The brightness of the two recorded peaks looks similar because the secondary burst overlaps with the declining brightness of the main meteor signal and, more important, due to the increasing distance of the meteor from the detector in this

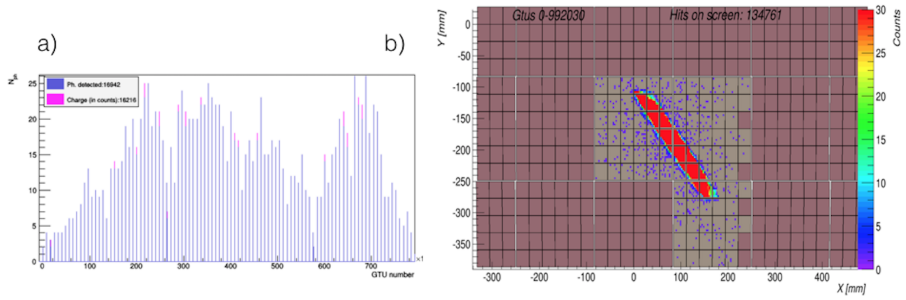

Figure 5: a) Expected light profile of a meteor of absolute magnitude $M = +5$ with the presence of a secondary burst. b) Meteor track on the focal surface by an event of magnitude $M = +5$ with light persistence phenomenon.

particular case.

The event including light persistence effects has been also simulated assuming an absolute magnitude $M = +5$. The assumed decay time was $\tau = 0.2\ s$ in this case. The persistence of the signal, which is not very evident in this case due to the moderate brightness of the simulated meteor, will be essential to derive the 3D trajectory and velocity of bright meteors, by exploiting the motion of the ISS.

The Mini-EUSO configuration has also been implemented in ESAF. Due to its much coarser pixel resolution (see table 3) Mini-EUSO will detect the light-curve with less intensity and spatial resolution. Fig. 6 shows an example of light signal and track detected by Mini-EUSO in case of a meteor with similar zenith angle and magnitude of the one shown in fig. 4 for JEM-EUSO.

5. EUSO-TA

First real observation of meteor events have been obtained using the EUSO-TA prototype on the ground. TA-EUSO is a complete prototype of the JEM-EUSO space telescope in operation since 2013 at the Telescope Array (TA) site in Black Rock Mesa, Utah, USA Kawai et al. (2008). The telescope can perform observations of ultraviolet light generated by cosmic-ray air showers and

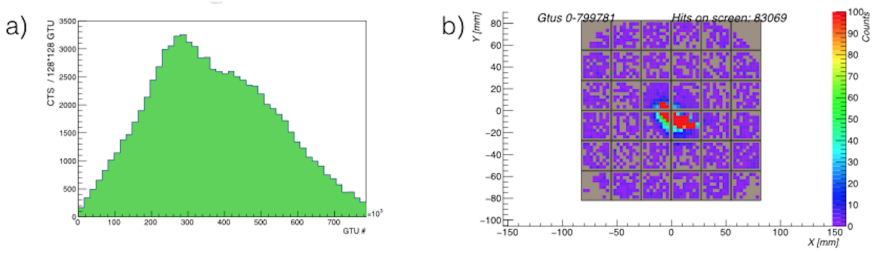

Figure 6: a) Expected light profile of a meteor of absolute magnitude $M = +5$ detected by Mini-EUSO. Each time bin on the x-axis correspond to 40.96 ms integration time. b) Expected track on the focal surface (no UV night glow light has been added yet).

Property	JEM-EUSO	Mini-EUSO	EUSO-TA
Pixel number	3.2×10^5	2304	2304
FOV at ground (km)	230	150	N/A
Full FOV	60°	40°	11°
Lenses diameter (m)	2.5	0.25	1.0
Pixel FOV	0.075°	0.8°	0.2°

Table 3: Comparison between JEM-EUSO, Mini-EUSO and EUSO-TA instrument parameters.

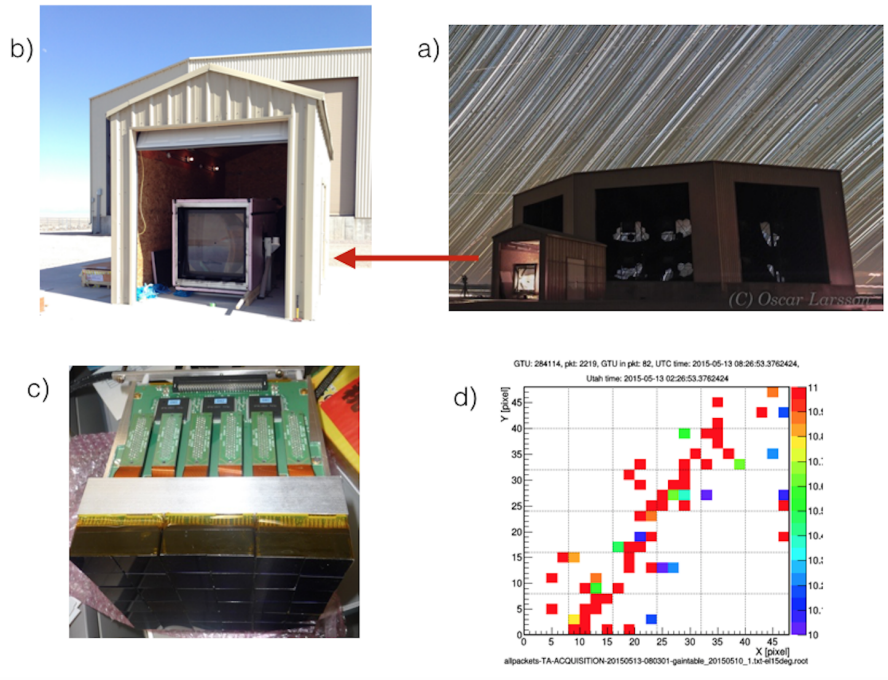

Figure 7: a) The TA fluorescence telescope at Black Rock Mesa with the EUSO-TA telescope in front. b) View of the EUSO-TA telescope with the front Fresnel lens. c) The PDM of the EUSO-TA telescope. d) Example of a cosmic ray track of energy E $\sim 10^{18}$ eV detected by EUSO-TA.

artificial sources. The aim of the project is to test the JEM-EUSO technology and to study the detector response in conjunction with the TA fluorescence detector.

The telescope is housed in a shed located in front of one of the fluorescence detectors of the Telescope Array collaboration (see Figs. 7a and 7b). The detector consists of two 1 m^2 sized square Fresnel lenses (see Fig. 7b) and the focal surface consists of one PDM equipped with 6 $\times$ 6 MAPMTs of 8 $\times$ 8 pixels (see Fig. 7c) with a field of view of 11° $\times$ 11° (FOV of $\sim$ 0.2° per pixel). The EUSO-TA apparatus is triggered externally by the TA experiment and images cosmic ray tracks. Fig. 7d shows a typical example. The signal lasts only 1 GTU, as the cosmic ray shower is detected very close to the apparatus

(less than 3 km). For this reason EUSO-TA can only record packets of 128 GTUs (for a total of 320 μs of data) with a maximum data rate of 20 Hz. In reality, as the typical trigger rate of TA is $\sim$3 Hz, only a few snapshots of any meteor track can be detected. In spite of this difficulty, so far 5 meteor events have been detected. Fig. 8 shows an example of such events. Plot (a) in this figure shows the integrated number of counts in each pixel. A 3σ threshold has been applied on each pixel to exclude almost all signals not due to the meteor track. Plots from (b) to (e) show the total number of counts of the meteor track detected by boxes of 5×5 pixels in the FOV in four consecutive packets. The discontinuity of the signal between packets is due to the discontinuity in which data are acquired. The time difference between the first and the last packet is about 1s. The apparent magnitude of this event is evaluated to be $m \approx 2.5$ (see caption of Fig. 8).

Despite the limited amount of information collected for these events, the above figure shows an experimental example on how meteor events would be imaged. An upgrade of EUSO-TA electronics and data acquisition is in progress, by including also a meteor trigger to follow continuously the time evolution of the meteor signal in the FOV of EUSO-TA.

6. Conclusions

The analysis presented in Adams et al. (2015d) already showed that JEM-EUSO has the capability to observe meteors down to magnitude $M = +7$. This result is supported by more detailed simulations performed by using the ESAF simulation code. Taking advantage of its large field of view and high detection rate, JEM-EUSO is able to record a statistically significant flux of meteors as a function of their magnitudes, both for what concerns sporadic meteors, and in cases of a variety of possible meteor streams. Unaffected by adverse weather conditions, which limit the effectiveness of ground-based meteor observation networks, JEM-EUSO will become a very important facility in the field of meteor studies. A particularly important role can be played in the detection of bright

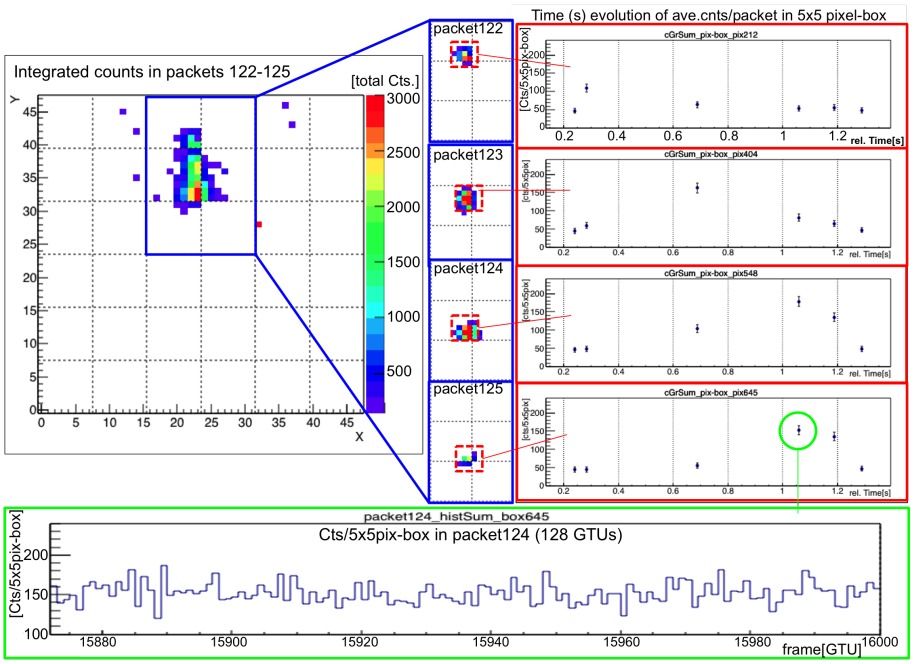

Figure 8: Meteor track detected by EUSO-TA. The integrated counts corresponding to the whole event are shown in the left. The panels on the right show the light profile of four different blocks of 5 × 5 pixels. The morphology of the event shows a fast initial brightening of about 0.9 mag, followed by a slightly slower decline of about 1.7 mag. The measurement is affected by several uncertainties, mainly due to the fact that part of the flux can be lost over non-sensible regions of the detector (zones between different PMTs). We can roughly estimate the magnitude of the meteor at maximum brightness, by computing differences of flux with respect to four different stars in the FOV. Taking into account all the uncertainties, including those related to the conversion of the star magnitudes, given in B colour, we can conclude that this meteor reached a magnitude of about 2.5. The panel on the bottom shows for a specific measurement, indicated by a circle in the plot above, the GTU by GTU evolution of the signal.

meteors and fireballs, as these events can be detected even during periods of very high sky background. Therefore, monitoring of these events can always be active, whereas the detection of faint meteors requires more optimal observing conditions.

An exciting development, though limited to sufficiently bright meteors, is the possibility to exploit the persistence of the meteor signal and the movement of the ISS to obtain a 3D reconstruction of the meteor trajectory and velocity, making it possible to compute the original heliocentric orbit of the meteoroid, a very important result for solar system studies.

Our preliminary analysis concerning the possible detection of nuclearites indicates that JEM-EUSO will be sensitive to nuclearites having masses higher than a few 10^{22} GeV/c^2. In addition, after a JEM-EUSO data acquisition time of only 24 hours, it will be able to provide limits on the possible nuclearite flux one order of magnitude lower than the limits reached by the experiments carried out so far.

Prior to JEM-EUSO, the Mini-EUSO pilot mission is expected to fly aboard the ISS on 2017-2018. It will prove the JEM-EUSO observational principle and by means of detailed offline data analysis it will allow us to detect meteors having magnitude as faint as absolute magnitude $M < +5$. Mini-EUSO will be sensitive to nuclearites with mass higher than a few 10^{24} GeV/c^2. After one month of operations it could reach a sensitivity of about 2 orders of magnitude better than what has been obtained so far by means of ground experiments.

A ground-based pathfinder mission of JEM-EUSO, named EUSO-TA, is in operation since 2013 in Utah. Despite the fact that the detector is specifically designed to be sensitive to cosmic rays events, a few meteor events have been observed so far, proving on ground the observational principle of JEM-EUSO. There are plans to equip in near future EUSO-TA electronics with a meteor trigger in order to track more clearly this category of events.

7. Acknowledgements

This work was partially supported by Basic Science Interdisciplinary Research Projects of RIKEN and JSPS KAKENHI Grant (22340063, 23340081, and 24244042), by the Italian Ministry of Foreign Affairs and International Cooperation, by the 'Helmholtz Alliance for Astroparticle Physics HAP' funded by the Initiative and Networking Fund of the Helmholtz Association, Germany, and by Slovak Academy of Sciences MVTS JEM-EUSO as well as VEGA grant agency project 2/0076/13. Russia is supported by the Russian Foundation for Basic Research Grant No 13-02-12175-ofi-m. The Spanish Consortium involved in the JEM-EUSO Space Mission is funded by MICINN & MINECO under the Space Program projects: AYA2009-06037-E/AYA, AYA-ESP2010-19082, AYA-ESP2011-29489-C03, AYA-ESP2012-39115-C03, AYA-ESP2013-47816-C4, MINECO/FEDER-UNAH13-4E-2741, CSD2009-00064 (Consolider MULTIDARK) and by Comunidad de Madrid (CAM) under projects S2009/ESP-1496 & S2013/ICE-2822.

References

J.H. Adams Jr. et al. (JEM-EUSO Collaboration), Exp. Astronomy, 40, 3 - 17 (2015).

J.H. Adams Jr. et al. (JEM-EUSO Collaboration), Exp. Astronomy, 40, 301 - 314 (2015).

J.H. Adams Jr. et al. (JEM-EUSO Collaboration), Exp. Astronomy, 40, 239 - 251 (2015).

J.H. Adams Jr. et al. (JEM-EUSO Collaboration), Exp. Astronomy, 40, 253 - 279 (2015).

Ambrosio, M., et al. (MACRO Coll.), Eur. Phys. J. C, 13 (2000) 453.

C. Berat et al., Astroparticle Physics, 33, 221 - 247 (2010).

M. Bertaina et al. (JEM-EUSO Coll.), Advances in Space Research, 53, 1515 - 1535 (2014).

Cecchini, S., et al. (SLIM Coll.), Eur. Phys. J. C, 57 (2008) 525.

A. De Rujula and S.L. Glashow, S.L., Nature, 312, 734 737 (1984).

L. G. Jacchia, et al., Smithsonian Contr. to Astrophys., 25, (1967).

H. Kawai et al. (TA Coll.), Nuclear Physics B (Proc. Suppl.), 175-176, 221 - 226 (2008).

A. Nardelli, Meteor simulation in ESAF for the JEM-EUSO mission, Bachelor Thesis, Università Telematica Internationale Uninettuno (2014).

Pavalas, G. E., et al. (ANTARES Coll.), Proceedings of the 23^{rd} European Cosmic Ray Symposium, Moscow, 543 (2012).

Price, P. B., Phys. Rev. D, 38, 3813-3814 (1988).

M. Ricci et al. (JEM-EUSO Collaboration), PoS(ICRC2015), 599 (2015).

J.B. Robertson and Wendell G. Ayers, NASA Technical Note D-4312 (1968); http://ntrs.nasa.gov/archive/nasa/casi.ntrs.nasa.gov/19680007281.pdf